Arena, G., Groh, R., Brinkmeyer, A., Theunissen, R., Weaver, P., & Pirrera, A. (2017). *Adaptive air inlet for fluid flow control*. Paper presented at 21st International Conference on Composite Materials, Xi'an, China.

Peer reviewed version

ADAPTIVE AIR INLET FOR FLUID FLOW CONTROL

G. Arena, R.M.J. Groh, R. Theunissen, A. Brinkmeyer, P.M. Weaver, A. Pirrera

Bristol Composites Institute (ACCIS), Dept. of Aerospace Engineering, University of Bristol, Bristol, UK, gae.arena@bristol.ac.uk, www.bristol.ac.uk/composites

Keywords: Adaptive structures, Air inlet, Wind Tunnel, Composites, Buckling, Post-buckling

ABSTRACT

In this paper, we exploit structural instabilities and elastically nonlinear behaviour as an engineering tool for designing an adaptive air inlet for fluid flow control. The device includes a shape changing post-buckled composite plate, which regulates the inlet aperture of a connected duct by snapping in response to changes in the pressure field of a surrounding fluid. The post-buckling stresses of the composite plate induce the intrinsic capabilities required for multi-stable snap-through, while the post-buckled shape creates the aerodynamic pressure fields for actuation. These concepts are validated here by means of Fluid-Structure Interaction (FSI) simulations and wind tunnel experiments.

1 INTRODUCTION

The continuous development in smart devices, actuators, sensors and multi-functional materials is currently stimulating interest in morphing and shape-changing structures. Such structures allow for a better compromise between stiffness, weight and functionality [1–5]. Specifically, passively actuated adaptive structures do not rely on external actuators to re-configure their shape, which is particularly attractive when weight and flexibility are crucial design parameters [6–8].

In this paper, we propose conceptual design principles for a novel class of adaptive structures that provide both flow regulation and control. The inlet exhibits a set of adaptive responses to varying fluid flow conditions that are obtained by exploiting the nonlinear post-buckling behaviour of a preloaded composite plate supported at its extremities. For passive actuation and adaptation, the device relies on changes in the surrounding air pressure as the velocity of the fluid flow is changed.

A post-buckled structure is said to be multi-stable when it can take two or more equilibrium states for the same set of external loading conditions [9]. The most basic example is the classical Euler beam loaded in compression, which upon reaching a critical load, loses stability on the initially flat equilibrium path, thereby snapping transversally onto one of two possible sinusoidal shapes.

Such a post-buckled structure can exhibit a dynamic "snap-through" behaviour between its stable states when subjected to an external load. For example, let us consider the buckled beam shown in Figure 1a. The first buckled state and the symmetrically opposite configuration are connected by an equilibrium path, shown graphically in Figure 1b, where the magnitude of a centrally applied force is plotted against central displacement. In general, two different scenarios can be observed.

1. The top right plot shows the case of bistability, i.e. when the applied force reaches a critical value, the structure snaps into its second configuration, traversing a region of instability where the load decreases. The second configuration is stable even when the load is removed, because the load-displacement curve intersects the displacement axis.
2. Conversely, the bottom right graph of Figure 1b shows the snap-through behaviour of a monostable structure. In this case, the second state is not stable upon removal of the load. Hence, snap-back to the initial configuration occurs when the load is removed.

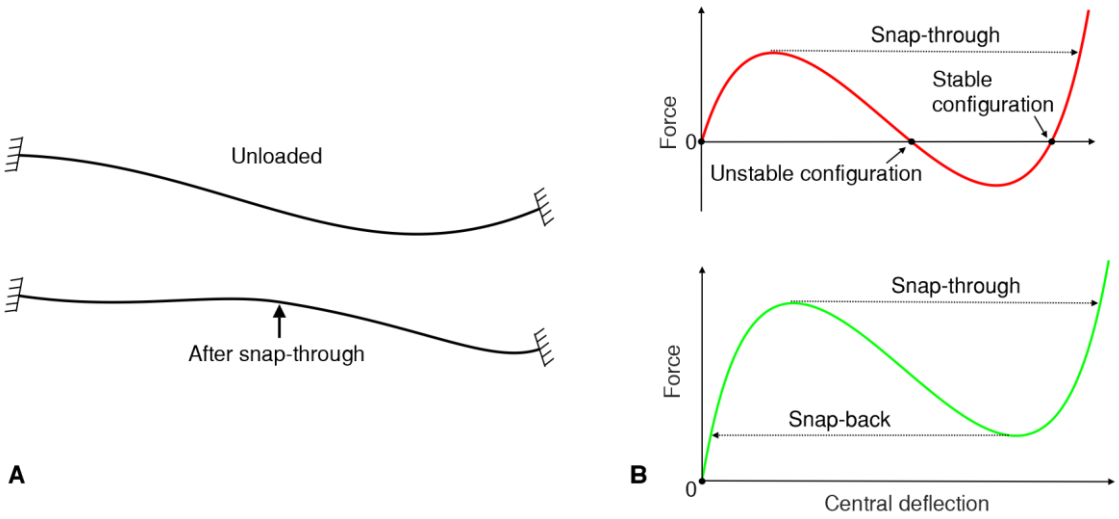

Figure 1. Buckled beam configurations before and after the "snap-through" (a). Force vs central deflection of a bi- and mono-stable structure (top and bottom, respectively) (b).

These two concepts are exploited here to design and manufacture an air inlet that, depending on applied boundary conditions, can either be mono- or bi-stable, where the force driving snap-through is the variation in pressure caused by the fluid flowing over the surface of the inlet. Fluid-Structure Interaction (FSI) simulations are carried out in the commercial software Abaqus to study the inlet's response to varying fluid flow conditions. The structural behaviour observed with the FSI results is successively validated by testing an adaptive multi-stable composite air duct in a high-speed wind tunnel.

2 FLUID-STRUCTURE INTERACTION MODELLING IN ABAQUS

Fluid-structure interaction is the study of the effect of a fluid on a structure, and vice versa. In these kind of problems, the pressure and velocity of the fluid influence, and are influenced by, the shape and possible displacements of the structure [10].

Abaqus/CEL is a recently released extension of Abaqus/Explicit. With this commercial tool, the interaction between fluid and structure is solved by means of contact constraints. A second approach to solve FSI problems in Abaqus, is the Arbitrary Lagrangian-Eulerian (ALE) formulation, which takes advantage of the coupling of Abaqus/CFD and Abaqus/Standard solvers [11], and is therefore also known as a "co-simulation".

The main difference between the two methods consists in the fluid discretisation, whereas the structural behaviour is analysed by means of a Lagrangian formulation in both cases. In particular, as shown in Figure 2, the fluid mesh in the ALE formulation tracks the structural deformation, which can lead to highly distorted fluid elements when extreme structural deformations occur. The Coupled Eulerian Lagrangian (CEL) formulation, on the other hand, is an "immersed boundary" technique [12], where a Lagrangian structure is immersed and free to move and deform through a fixed Eulerian fluid mesh. The Eulerian material tracking is governed by measuring the Eulerian volume fraction (EVF) in each mesh element. In particular:

- EVF = 1 if the element is completely filled with fluid.
- EVF = 0 if there is no material within a fluid element.
- 0 < EVF < 1 if the element is partly filled by fluid.

This approach reduces the computational cost as re-meshing is not required. The issue of high mesh deformation is also avoided.

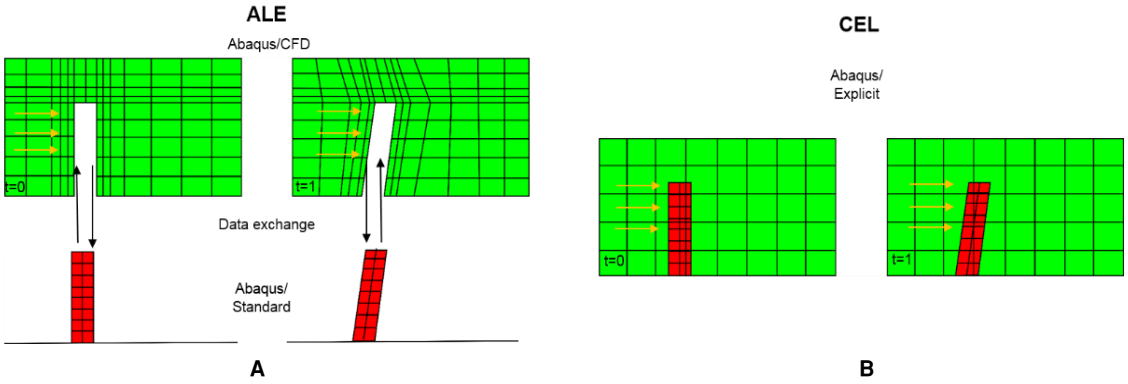

Figure 2. ALE Abaqus/standard-explicit co-simulation (a) compared with CEL method (b).

The second major difference between the two approaches is the FSI interface tracking method. The CEL uses the so-called volume of fluid (VOF) method [13], which applies a contact between fluid and structure when, at the specific interface node, the EVF arithmetic mean of the surrounding elements is higher the 0.5. If the mean EVF < 0.5, contact is not imposed. The disadvantage of this approach is that it can lead to "leakage" and inauthentic acceleration of the fluid [14]. The ALE method, on the other hand, applies kinematic and dynamic constraints at the fluid-structure boundaries [11].

The ALE method simulates the fluid dynamics by means of the Abaqus/CFD solver, which solves the incompressible form of the Navier-Stokes equations. Conversely, the CEL method uses an equation of state (EOS), relating pressure (p), density (ρ) and specific energy (Em), in combination with the compressible form of the Navier-Stokes equations [11].

For the problem considered here, the CEL approach is chosen for the following reasons:

- The extreme fluid and structure deformation occurring during the closure of the inlet will render the ALE co-simulation computationally very expensive due to the necessary re-meshing of the fluid volume at each time instant. In CEL on the contrary re-meshing is not required.
- Contact between different structural parts is not possible in the fluid mesh of the ALE model, as this would cause fluid elements to collapse. The adaptive air inlet studied here requires contact between the buckled multi-stable part and the inlet cover.

Considering the limitation of the CEL methods listed in this section and further elucidated in Ref. [11], experimental results are presented to validate the concepts shown.

3 METHODS

3.1 Multistable structure

A finite element model of the multistable adaptive inlet is constructed. The material chosen is a UD (uni-directional) glass fibre epoxy resin composite, Glass/913, with material properties as shown in Table 1. In order to induce not only bistable, but also monostable snap-though, the symmetry of the structure is broken by changing the thickness along the length of the composite, as shown in Figure 3. The structure is therefore composed of a minimum of three and a maximum of six layers, where each layer has a thickness of 0.13 mm, maximum length of 450 mm and width of 150 mm. Vertical displacement and precompression are applied to the last 50 mm of right end of the inlet. The former is kept fixed at 50 mm, while precompression of 6 mm or 7 mm is applied when either monostable or bistable snap-though is desired, respectively.

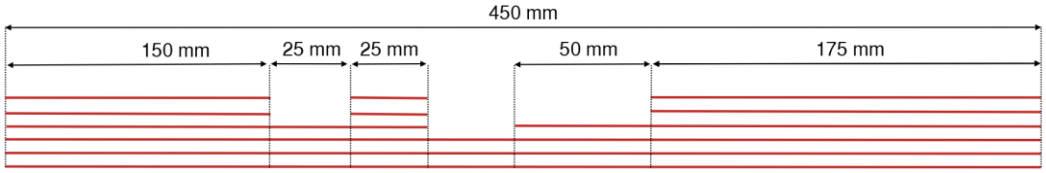

Figure 3. Composite layup for the multistable inlet with snap-through behaviour. Red lines represent composite layers. Step changes in thickness cause stiffness variations and the structural asymmetry required for monostable behaviour with snap-through.

Table 1. Glass/913 layer properties.

E1 [GPa]	E2 [GPa]	G12 [GPa]	ν12 [-]	Thickness [mm]
43.7	7.5	4.3	0.3	0.13

An 8-node linear brick element C3RD8R, with reduced integration and enhanced hourglassing control, is selected. A fine mesh with 12960 elements is required to ensure convergence of the non-linear post-buckling behaviour. In the thickness direction, one element for each layer is used.
As a preliminary study, the non-linear snap-through behaviour in the absence of surrounding fluid is evaluated with an arc-length Riks algorithm [15]. An explicit integration scheme is used, with an automatic, adaptive time-step. An isotropic elastic material with a Young's modulus of 2 GPa is used for the inlet cover.

3.2 Fluid Structure Interaction

Error! Reference source not found. shows the FSI model for the adaptive inlet. The green background represents the air in which the structure is immersed. Due to extreme deformations of both the structural and fluid domains, a Coupled Eulerian-Lagrangian (CEL) approach is chosen [10, 11] as discussed afore.

The CEL method combines the compressible form with an EOS of the type $p = f(\rho, Em)$. When using this method, the boundaries of the Eulerian domain will reflect pressure waves, causing an oscillating wave across the domain, which adversely affect the numerical solution. This problem is avoided by assigning a constant initial velocity field throughout the entire Eulerian domain, which represents steady state flow conditions. By choosing this option, the inlet velocity of the fluid domain cannot change during the simulation.

The air flowing over the structure is modelled as a Newtonian fluid, with density ρ = 1.205 kg/m^3 and viscosity μ = 1.82·10-5 Pa·s – the standard properties at 20 °C and atmospheric pressure [18]. CEL simulations, require a compressibility factor as an input. This is derived from the speed of sound in air, which is normally equal to c = 343 m/s at 20 °C. A gauge relative pressure P = 0 Pa is assigned beneath the air inlet where no fluid is assumed to flow. In order to avoid flow reversal, it is necessary to use a sufficiently long duct and/or impose a negative gauge relative pressure, P_{outlet}. It is important to note that the outlet pressure is a fundamental parameter that affects the structural behaviour and, consequently, its design. The inlet is designed for a snap-through velocity of about 30 m/s. This value is therefore imposed as the initial fluid velocity for the Eulerian mesh.

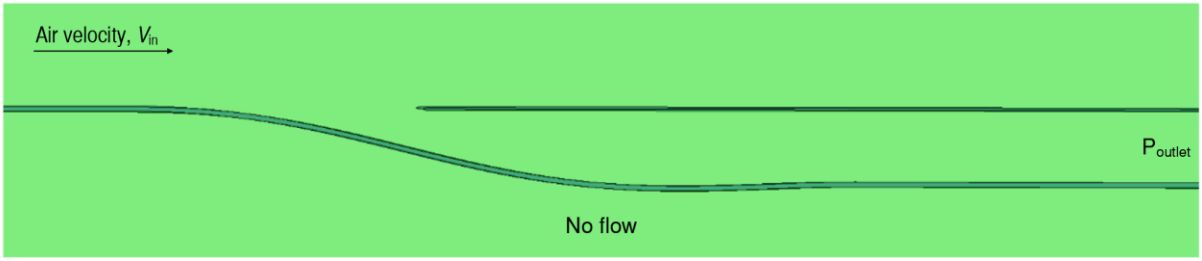

Figure 4. A portion of the computational domain for the Fluid-Structure Interaction model. Air flows from left to right.

A default penalty contact method manages the solid-solid interaction, while the so-called volume of fluid (VOF) method [13] is used for the fluid-solid interface tracking. The VOF method enforces the contact constraints and no-slip conditions when, at the specific interface nodes, the arithmetic mean of the EVF of the surrounding elements is higher than 0.5 [11].

Only one element is used through the width of the domain. The size of the fluid domain is chosen to be large enough (0.3 x 0.45 m) to minimise any boundary effects. For accuracy and convergence, the fluid mesh is refined homogeneously resulting in 700,000 8-node linear Eulerian brick elements of the type EC3D8R. The entire Eulerian domain is filled with air, so that the EVF is equal to 1 everywhere.

3.3 Wind tunnel experiments

Experiments in the Low Turbulence Wind Tunnel at the University of Bristol are carried out to validate the FSI simulations. This wind tunnel is able to reach speeds up to 80m/s while maintaining turbulence intensity levels in the order of 0.09%. The experiments allow in addition to possibly unearth further interesting behaviours of the inlet, especially because the full complexity of the fluid-structure interaction can be complicated to model due to method limitations, as described in Section 2 and 3.2, and/or computational costs.

An adaptive air inlet, illustrated in Figure 5, was designed and manufactured. The main component consists of a multi-stable composite plate designed using the FE buckling and post-buckling study described in Section 3.1. The structure is composed of three to six plies of conventional E-glass reinforced epoxy matrix UD prepreg (HexPly 913G-E-5-30% supplied by Hexcel) with 0.13 mm nominal cured thickness, 192 g/m2 glass fiber mass per unit area and 30% mass (~40% volume) cured resin content. Mechanical properties are shown in Table 1. The obtained UD layup, with a ply sequence shown in Figure 3, is cured with a vacuum bagging technique at a temperature of 125 °C and pressure of 1 bar for 60 min. A heat up rate of 2 °C was chosen.

Figure 5b, c and d show in detail the mechanism and connected components used to apply vertical displacement and pre-compression to buckle the composite panel and achieve the desired post-buckling behaviour. One extremity of the composite plate (1) is clamped to a 10 mm thick Polymethylmethacrylate (PMMA) plate, which is bolted on the floor of the wind tunnel. The other end of the inlet is connected through an opening in the PMMA plate to an aluminum support (9) placed immediately underneath the wind tunnel floor. This way the difference in height between the two composite extremities is exactly 50 mm. Precompression is imposed by a simple linear mechanism: the handwheel's (5) rotation applies torsion to a TR 20x4 D steel trapezoidal lead-screw (7) that converts rotational motion to linear displacement by means of a KSM 20x4 bronze flanged trapezoidal nut (10) fixed to the aluminum support. A controlled and smooth linear movement is guaranteed by the HIWIN HGW20CCZ linear carriages (11) and HGR20RH-500 rails (13) on which the support is fixed. Compressive displacement is measure by the encoder (12) of HIWIN MAGIC PG positioning measurement system. The lead-screw, nut, support bearings and HIWIN linear systems were provided by Moore International LTD. PMMA lateral walls (6) are placed next to the inlet edges in order to drive the airflow above the composite and allow the air to flow out through an outlet channel (14) 200 mm in length. The manufactured air inlet is placed on the floor of the 0.8 m x 0.6 m octagonal section of the Low Turbulence Wind Tunnel. Six pressure taps are placed on the back side of the composite plate and connected to a MicroDaq Pressure Scanner.

The initially stable configuration of the composite plate maintains an open aperture of the air inlet. The deformable structure then snaps into a second "closed" configuration as the fluid velocity is increased. The second state can either be self-equilibrated meaning that the inlet will remain closed even when the air ceases to flow (bistability), or the plate can return to its open configuration once the fluid flow is stopped (monostability).

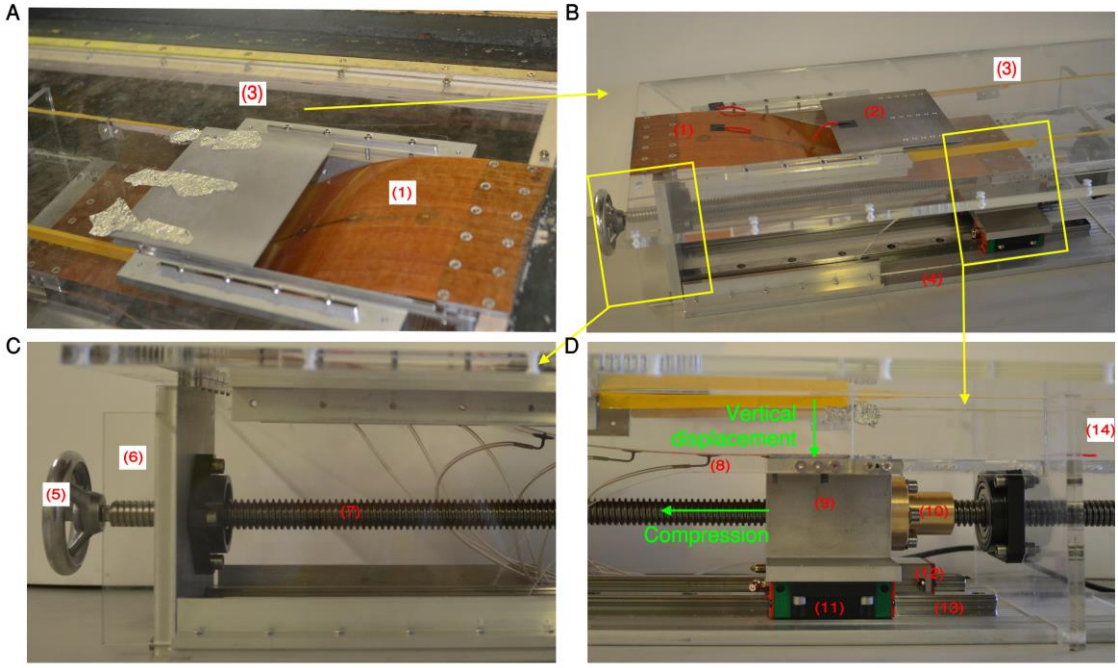

Figure 5. Air inlet mechanism placed in the wind tunnel facility (a). One of the morphing composite inlet (1) extremities is clamped to the PMMA plate (3) on the wind tunnel floor. Air flows through the duct to the bottom on the tunnel. On the top right side (b), the entire model is shown, while, on the bottom, left (c) and right (d) details are depicted. The whole mechanism is composed of: (1) morphing composite inlet; (2) adjustable cover tap; (3) PMMA plate; (4) aluminum bottom plate; (5) handwheel; (6) PMMA lateral walls; (7) trapezoidal lead-screw; (8) pressure taps; (9) aluminum right support; (10) bronze trapezoidal flanged nut; (11) Hiwin carriage; (12) encoder for linear measuring system; (13) Hiwin linear rails; (14) outlet channel.

4 RESULTS

4.1 Fluid Structure Interaction

Error! Reference source not found. shows the transverse force *vs* central deflection curves for the structure, when a vertical displacement of 50 mm and pre-compression either of 7 mm (**Error! Reference source not found.**a) or 6 mm (**Error! Reference source not found.**b) are applied at the right extremity. In both cases the composite exhibits snap-through behaviour, but with different loading-unloading paths. As expected, with higher pre-compression the structure behaves as bistable panel and has a second stable configuration in its unloaded state. By decreasing the precompression to 6 mm, the structure snaps back to its open state upon removal of the transverse load.

The effect of the aerodynamic loads on the bistable adaptive inlet is shown in **Error! Reference source not found.**. The structure is immersed into a 30 m/s airflow creating a negative pressure field over the inlet sufficiently low to actuate snap-through of the composite to the closed configuration. **Error! Reference source not found.**d shows that the inlet maintains its second stable state even when air ceases to flow into the channel. Similarly, the inlet with lower precompression, *i.e.* in a monostable layout, reacts to the airflow by snapping to its second configuration, which is maintained until the air speed decreases below a critical threshold. At this lower velocity, snap-back occurs and the air can flow into the inlet once again. It is worth noting that the force needed to actuate snap-though is higher than the force required to prevent snap-back (Figure 6b); approximately 0.015N vs 0.006N. This means that the negative pressure, and accordingly the air velocity, required to close the inlet will be higher than the negative pressure (velocity) at which the snap-back occurs.

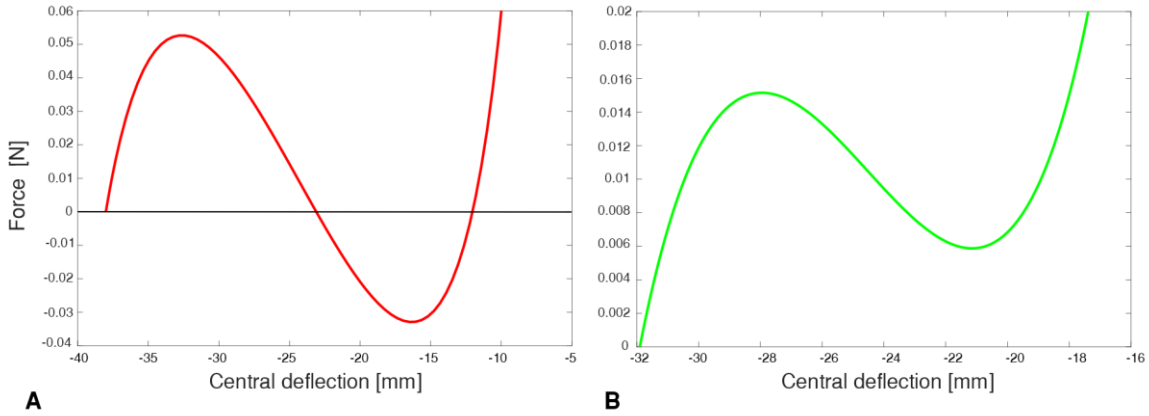

Figure 6. Snap-through behaviour of the bi-stable inlet when 7 mm of precompression is applied (a). Snap-through behaviour of the mono-stable inlet when 6 mm of precompression is applied (b)

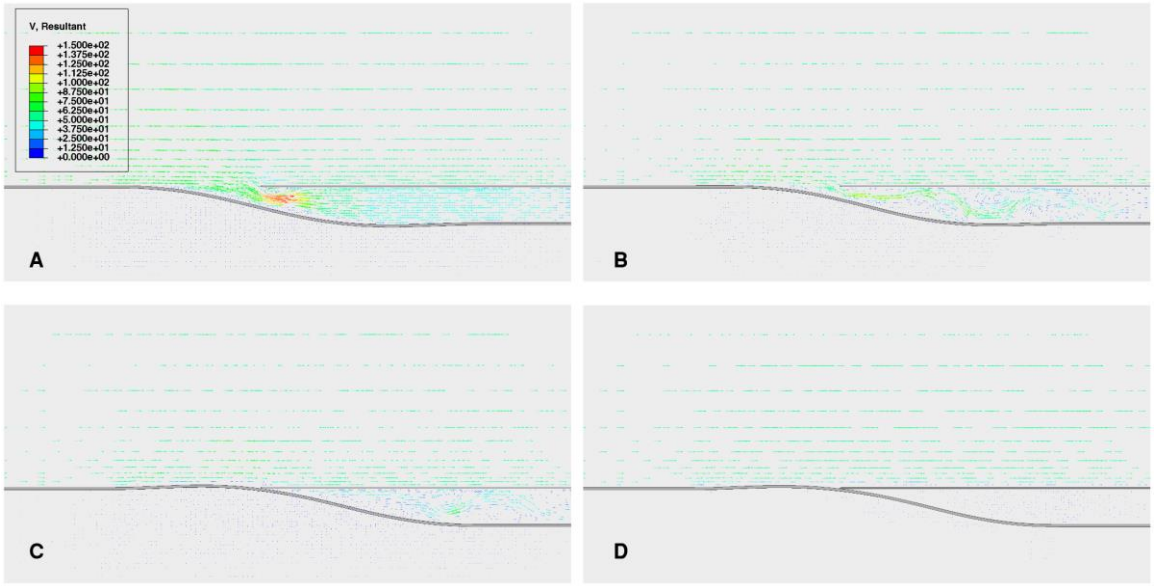

Figure 7. Passive actuation of a multistable adaptive air inlet. A 60 m/s air flow above the inlet causes a pressure field actuating snap-through from the initially open state to the closed state. The bistable configuration holds its closed configuration even when the air flow ceases due to its structural characteristics. The monostable configuration inlet (not shown) shows similar behaviour, but the closed configuration is not stable with respect to decreasing air speeds. Colored arrows represent the velocity vector field, with minimum and maximum magnitude speeds indicated in blue and red, respectively. From open to closed state the snap-through takes of the order of 10 ms.

As mentioned in Section 3.2, in order to avoid boundary reflections in the simulations, a constant predefined velocity is assigned to each node of the Eulerian fluid domain above the inlet. This setting, which is essential to achieve convergence of the analysis, prevents variations in the fluid domain inlet velocity during the simulation. For this reason, further adaptive inlet responses were demonstrated by means of experimental validation.

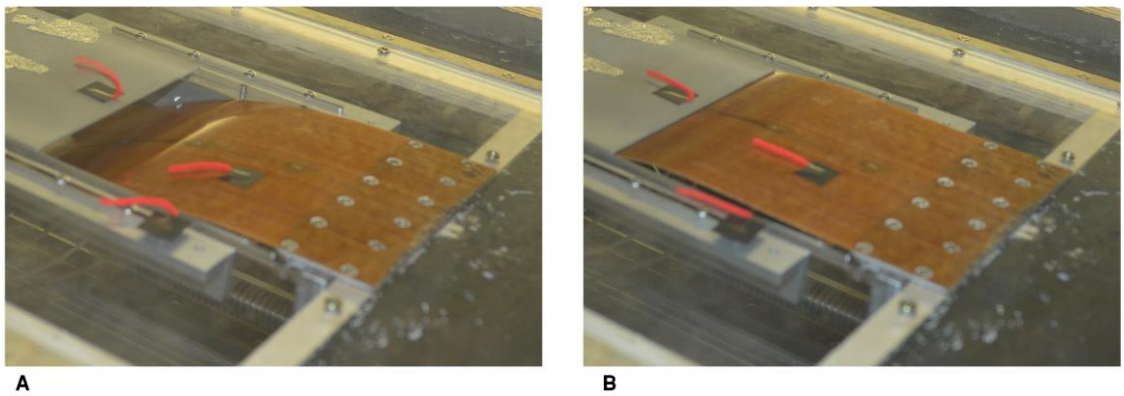

Figure 8. Adaptive composite inlet in the Wind Tunnel facility. Inlet in its stable open configuration (a) and in its stable/unstable closed configuration (b).

4.2 Wind tunnel experiments

The experiment starts by applying pre-compression to the lower extremity of the inlet, 7 mm to achieve bistabilty and 6 mm to achieve monostability. The airflow speed is regulated to gradually increase from 5 m/s to 25 m/s and then gradually decrease to 0 m/s. Figure 8a shows the adaptive inlet in its first open configuration. Snap-through into the closed state, as shown in Figure 8a, occurs around 20 m/s in the case of bistability and around 17 m/s in the case of monostability. As expected, the bistable inlet maintains its closed configuration despite decreasing air speed to 0 m/s, whereas, the monostable inlet snaps back when air velocity is lowered to 10 m/s. It was observed that a "valve-like" behaviour can be obtained by periodically increasing and decreasing air speed between 10 and 17 m/s.

5 DISCUSSION AND CONCLUSIONS

Passively actuated devices have the unique capability of property adaptation in response to changing environmental and/or operating conditions. Adaptive structures that do not rely on additional actuators to adjust their configuration guarantee higher functionality without incurring a weight penalty or loss of stiffness.

In this work, structural instabilities and effects of different boundary conditions on buckling and post-buckling behaviour, are exploited as an engineering design tool for an adaptive multistable air inlet. It is shown that the same post-buckled panel can be designed to be either bistable or monostable, simply by decreasing the applied precompression from 7 to 6 mm.

These concepts are used to design and manufacture a shape-changing air duct. FSI simulations and wind tunnel experiments are carried out to study the adaptive response of the device when immersed in airflow.

FSI simulations, carried out with a CEL approach in Abaqus, and experimental results showed that air flowing above the structure induces pressure fields that actuate snap-through of the inlet in both the bistable and monostable cases. Specifically, the wind tunnel experiments confirmed that the bistable inlet holds the closed configuration when the air speed is decreased to 0 m/s. On the other hand, the monostable structure snaps-back when the air speed is decreased below 10 m/s. This result can be exploited to achieve a "valve-like" behaviour by periodically increasing and decreasing air speed.

6 REFERENCES

[1] D. Wagg, I. Bond, P. Weaver, and M. Friswell, *Adaptive Structures*. Chichester: John Wiley & Sons, 2007.

[2] L. F. Campanile, "Initial Thoughts on Weight Penalty Effects in Shape-adaptable Systems," *J.*

Intell. Mater. Syst. Struct., vol. 16, no. 1, pp. 47–56, 2005.

[3] B. Sanders, D. Cowan, and L. Scherer, "Aerodynamic Performance of the Smart Wing Control Effectors," *J. Intell. Mater. Syst. Struct.*, vol. 15, no. 4, pp. 293–303, 2004.

[4] T. Yokozeki, S. Takeda, T. Ogasawara, and T. Ishikawa, "Mechanical properties of corrugated composites for candidate materials of flexible wing structures," *Compos. Part A Appl. Sci. Manuf.*, vol. 37, no. 10, pp. 1578–1586, 2006.

[5] T. a. Weisshaar, "Morphing Aircraft Systems: Historical Perspectives and Future Challenges," *J. Aircr.*, vol. 50, no. 2, pp. 337–353, 2013.

[6] A. K. Stowers and D. Lentink, "Folding in and out: passive morphing in flapping wings," *Bioinspir. Biomim.*, vol. 10, no. 2, p. 025001, Mar. 2015.

[7] G. Senatore, P. Duffour, S. Hanna, and F. Labbe, "Pumping vs. Iron: Adaptive Structures for Whole Life Energy Savings," in *2011 Seventh International Conference on Intelligent Environments*, 2011, pp. 114–121.

[8] A. F. Arrieta, I. K. Kuder, M. Rist, T. Waeber, and P. Ermanni, "Passive load alleviation aerofoil concept with variable stiffness multi-stable composites," *Compos. Struct.*, vol. 116, pp. 235–242, 2014.

[9] S. P. Timoshenko, *Theory of elastic stability*. Courier Corporation, 1970.

[10] H.-J. Bungartz and M. Schäfer, *Fluid-Structure Interaction. Modelling, Simulation, Optimization*. München: Springer, 2006.

[11] Dassault Systèmes (SIMULIA), *Abaqus Documentation*, 6.14 ed. Paris, France, 2016.

[12] A. M. Bavo, G. Rocatello, F. Iannaccone, J. Degroote, J. Vierendeels, and P. Segers, "Fluid-Structure Interaction Simulation of Prosthetic Aortic Valves : Comparison between Immersed Boundary and Arbitrary Lagrangian-Eulerian Techniques for the Mesh Representation," *PLoS One*, 2016.

[13] C. W. Hirt and B. D. Nichols, "Volume of fluid (VOF) method for the dynamics of free boundaries," *J. Comput. Phys.*, vol. 39, no. 1, pp. 201–225, 1981.

[14] A. Sillem, "Feasibility study of a tire hydroplaning simulation in a finite element code using a coupled Eulerian-Lagrangian method," 2008.

[15] E. Riks, "An Incremental Approach to the Solution of Snapping and Buckling Problems," *Int. J. Solids Struct.*, vol. 15, pp. 529–551, 1979.

[16] K. Williams, G. T. Chiu, and R. Bernhard, "Adaptive-passive absorbers using shape-memory alloys," *J. Sound Vib.*, vol. 249, no. 5, pp. 835–848, 2002.

[17] W. F. Noh, "CEL: A time-dependent, two space dimensional, coupled Eulerian–Lagrangian code," *Methods Comput. Phys. 3*, pp. 117–179, 1964.

[18] I. O. for Standardization, "ISO Standard Atmosphere." 1972.

ACKNOWLEDGEMENTS

We are grateful to Clint Davies-Taylor and the SIMULIA UK technical team for their support. This work was supported by the U.K. Engineering and Physical Sciences Research Council (EPSRC) through grants number EP/M013170/1 and EP/M507994/1.